Surface formation of HCOOH at low temperature

S. Ioppolo,[1]⋆ H. M. Cuppen,[1,2] E. F. van Dishoeck[2,3] and H. Linnartz[1]

[1]*Raymond & Beverly Sackler Laboratory for Astrophysics, Leiden Observatory, Leiden University, PO Box 9513, 2300 RA Leiden, the Netherlands*
[2]*Leiden Observatory, Leiden University, PO Box 9513, 2300 RA Leiden, the Netherlands*
[3]*Max-Planck-Institut für Extraterrestriche Physik, Giessenbachstrasse 1, D-85741 Garching, Germany*

ABSTRACT

The production of formic acid (HCOOH) in cold and hot regions of the interstellar medium is not well understood. Recent gas-phase experiments and gas-grain models hint at a solid-state production process at low temperatures. Several surface reaction schemes have been proposed in the past decades, even though experimental evidence for their efficiency was largely lacking. The aim of this work is to give the first experimental evidence for an efficient solid-state reaction scheme providing a way to form HCOOH under astronomical conditions. Several surface reaction channels have been tested under fully controlled experimental conditions by using a state-of-the-art ultrahigh vacuum set-up through co-deposition of H atoms and $CO:O_2$ mixtures with 4:1, 1:1 and 1:4 ratios. During deposition spectral changes in the ice are monitored by means of a Fourier transform infrared (FTIR) spectrometer in reflection absorption infraRed (RAIR) mode. After co-deposition a temperature programmed desorption (TPD) experiment is performed and gas-phase molecules are detected by a quadrupole mass spectrometer (QMS). Formation of HCOOH is observed at low temperatures mainly through hydrogenation of the HO–CO complex, while reactions with the HCO radical as intermediate are found to be inefficient. The HO–CO complex channel, which was previously not considered as an important HCOOH formation route, can explain the presence of HCOOH in dense cold clouds, at the beginning of the warm-up phase of a protostar, and, therefore, is likely to be astrochemically relevant.

Key words: astrochemistry – methods: laboratory – ISM: atoms – ISM: molecules – infrared: ISM.

1 INTRODUCTION

Formic acid (HCOOH), the smallest organic acid, has been observed in the past decades towards high- and low-mass star-forming regions and quiescent clouds in the gas phase (e.g. Zuckerman, Ball & Gottlieb 1971; Winnewisser & Churchwell 1975; Dishoeck et al. 1995; Gibb et al. 2000b; Ikeda et al. 2001; Liu, Mehringer & Snyder 2001; Liu et al. 2002; Requena-Torres et al. 2006; Bisschop et al. 2007c; Bottinelli et al. 2007), and likely also in the solid phase (e.g. Schutte et al. 1998, 1999; Gibb et al. 2000a, 2004; Boogert et al. 2004, 2008; Knez et al. 2005).

Despite the detection of HCOOH in a variety of interstellar environments, its astrochemical origin is still unclear. Leung, Herbst & Huebner (1984) discussed in their gas-phase model that HCOOH can be formed in dense interstellar clouds through the dissociative recombination of protonated formic acid ($HCOOH_2^+$), which forms by radiative association of HCO^+ and H_2O. Irvine et al. (1990) reported a detection of HCOOH in L134N with a relative abundance with respect to H_2 of 10^{-10}. They attributed the formation of HCOOH in this cold dark cloud to the ion-molecule gas-phase reaction $CH_4 + O_2^+$ followed by a dissociative recombination of protonated formic acid. According to Vigren et al. (2010), who combined a laboratory study and a gas-phase model, dissociative recombination of protonated formic acid is not as efficient as previously thought and the branching ratio of the channel leading to HCOOH has a maximum of only ∼13 per cent. Therefore, they suggested that HCOOH is *predominantly* formed in dense interstellar clouds through surface reactions on grains, even though experimental evidence for the efficiency of surface reactions is largely lacking.

Several solid-phase reaction channels have been proposed in the past decades. Tielens & Hagen (1982) included in their astrochemical model the formation of solid HCOOH on grain surfaces through successive addition of H, O and H to CO ice:

$$CO + H \rightarrow HCO \xrightarrow{O} HCO_2 \xrightarrow{H} HCOOH. \tag{1}$$

⋆E-mail: ioppolo@strw.leidenuniv.nl

As suggested by Garrod & Herbst (2006), HCOOH could also be formed through the solid-state reaction:

$$HCO + OH \rightarrow HCOOH. \tag{2}$$

In a recent laboratory study, Öberg et al. (2009) investigated, among others, reactions (1) and (2) experimentally by ultraviolet processing of CH_3OH-rich containing ices in which both HCO and OH are produced. However, only upper limits on HCOOH are found in this study. The alternative route of direct hydrogenation of solid CO_2 was tested by Bisschop et al. (2007b), who did not detect any HCOOH formation at low temperatures (below 15 K).

In this work an alternative formation route is studied in detail. Goumans, Uppal & Brown (2008) investigated the formation of CO_2 on a carbonaceous surface representing a model grain with density functional theory. According to their calculations the surface reaction CO + OH can yield a HO–CO complex, stabilized by intramolecular energy transfer to the surface. This intermediate can subsequently react, in a barrierless manner, with an H atom to form $CO_2 + H_2$, $H_2O + CO$ or HCOOH. Which of these three schemes is followed appeared to depend only on the orientation of the HO–CO intermediate and the incoming hydrogen atom. Therefore, the authors postulated that statistically about one third of the events will form HCOOH. We will experimentally focus on solid HCOOH formed through the latter route:

$$CO + OH \rightarrow HO\text{–}CO \xrightarrow{H} HCOOH. \tag{3}$$

This paper is organized according to the following experimental procedure. Starting from hydrogenation of simple molecules, like CO and O_2, we investigate efficiency and branching ratios of this surface reaction route. Simultaneous deposition (co-deposition) of H atoms and $CO:O_2$ mixtures with a selected ratio allows us to control the hydrogenation level and composition of the ice. Therefore, under our experimental conditions, radicals trapped in a $CO:O_2$ matrix are available for further reactions upon heating of the ice (Section 2). Infrared (IR) spectroscopy and mass spectrometry are combined to constrain the experimental results and to detect the formed and intermediate species (Section 3). Our experiments are not designed to simulate a realistic interstellar ice, but to test the above reactions. They provide information which can subsequently be included in astrochemical models of interstellar clouds. Specifically, we discuss the astrophysical importance of this reaction as an efficient channel for HCOOH formation at low temperatures (10–20 K) in the dense interstellar clouds (Section 4).

2 EXPERIMENTAL PROCEDURE

The experimental set-up (SURFRESIDE) has been described in detail elsewhere by Fuchs et al. (2009) and Ioppolo et al. (2010). Here we give a brief description of the apparatus, focusing more on the experimental procedure. H atoms are deposited together with CO and O_2 molecules (co-deposition) on a gold coated copper substrate, placed in the centre of the ultrahigh vacuum main chamber (10^{-10} mbar). $CO:O_2$ mixtures with a ratio of 4:1, 1:1 and 1:4 are prepared in a high-vacuum glass line, which comprises a liquid nitrogen trap to prevent water pollution. During the co-deposition the substrate is kept at a temperature of 15 K by a close-cycle He cryostat with a relative temperature precision of 0.5 K and an absolute accuracy better than 2 K. Deposition of the mixtures occurs under an angle of $45°$ with a flow of 5×10^{-8} mbar, while the H-atom beam is normal to the sample.

H atoms are supplied by a well-characterized thermal cracking source (Tschersich & von Bonin 1998; Tschersich 2000; Tscher-

sich, Fleischhauer & Schuler 2008). H_2 molecules are cracked in a capillary pipe surrounded by a tungsten filament, which is heated to 2200 K. During the H-atom exposure, the pressure in the atomic line is kept constant at 1×10^{-6} mbar. Hot H atoms are cooled to room temperature via collisions by a nose-shaped quartz pipe, placed in the H-atom beam path. The geometry of the pipe is designed in such a way that each H atom has at least four collisions with the walls before leaving the pipe. In this way, hot species (H; H_2) cannot reach the ice directly. Furthermore, previous experiments with liquid nitrogen cooled atomic beams did not show any H/D-atom temperature dependence in hydrogenation reaction processes (e.g. Watanabe et al. 2006; Miyauchi et al. 2008; Oba et al. 2009). The final H-atom flux (2.5×10^{13} atoms cm^{-2} s^{-1}) is measured at the substrate position in the main chamber using a Quadrupole Mass Spectrometer (QMS), as described in the appendix of Ioppolo et al. (2010). The absolute error in the H-atom flux determination is within 50 per cent.

The ice is monitored by means of reflection absorption infrared (RAIR) spectroscopy, using a Fourier transform infrared spectrometer (FTIR). The FTIR covers the range between 4000 and 700 cm^{-1} (2.5–14 µm) with a spectral resolution of 1 cm^{-1} and a co-addition of 128 scans. RAIR difference spectra (ΔA) with respect to the bare 15 K gold substrate spectrum are acquired every few minutes during the experiment. The QMS that monitors gas-phase species is placed behind the substrate and in line with the HABS. Following all our co-deposition experiments a temperature programmed desorption (TPD) is performed by heating linearly the co-deposited ice to 200 K with a rate of 0.5 K min^{-1}. Each separate experiment is performed twice to link the RAIRS to the QMS data: during the first experiment the sample is kept in the IR optical line also during the TPD phase; in the second experiment the sample is turned $180°$ to face directly the QMS after co-deposition.

The main goal of this work is to improve our qualitative picture of possible reaction schemes and to search for an efficient HCOOH formation channel that may be responsible for the observed abundances of HCOOH in quiescent clouds. To enhance the detection of intermediates in the reaction schemes, we carry out a so-called co-deposited experiment in which hydrogenation occurs while the mixture is deposited. Moreover, since a beam of OH radicals and a H-dominated environment is difficult to produce, we use a mixture of CO with O_2, because hydrogenation of O_2 ice is known to lead to efficient OH production (Cuppen et al. 2010; Ioppolo et al. 2010). The ratio between H atoms and $CO:O_2$ mixtures during co-deposition at 15 K determines the hydrogenation grade in our experiments. We are interested in the CO and O_2 dominated regime, where full hydrogenation is not reached and radicals are trapped in the ice. Thus, the same $H/[CO:O_2] = 2$ ratio is applied to all the H and $CO:O_2$ co-deposition experiments, resulting in a deposited ice mainly consisting of CO and O_2 molecules. RAIRS and QMS results from the co-deposition experiments are compared to those from selected control experiments in order to give experimental evidence for the unambiguous solid HCOOH formation under our laboratory conditions. For this purpose, pure HCOOH and H_2CO ices and mixtures of $H_2O:HCOOH$ and $H_2O:H_2CO$ (10:1 and 3:1, respectively) are used as control experiments. The HCOOH containing ices are deposited at 30 K, while the H_2CO containing ices are formed *in situ* by hydrogenation of several thin layers (1 monolayer (ML) per step) of pure CO ice or $H_2O:CO$ mixtures at 12 K. The hydrogenation is stopped once almost all the CO is converted into H_2CO ice: the H_2CO formation yield has reached its maximum at this point and only traces of CH_3OH ice are formed, as shown by Fuchs et al. (2009).

## 3 RESULTS AND DISCUSSION

3.1 Formation of solid HCOOH

Fig. 1 shows the normalized TPD curves obtained by the QMS with a rate of 0.5 K min^{-1} for the 46 amu (HCOOH) and 30 amu (H$_2$CO) mass signals from the H-atom and CO:O$_2$ = 4:1 co-deposition experiment compared to the normalized and offset TPD curves of selected control experiments to prove unambiguously the formation of HCOOH ice. Mass 46 amu (left-hand column) from the co-deposition experiment has a broad desorption peak at ~160 K in the TPD curve with a low signal-to-noise ratio, due to the weakness of this peak before normalization (Fig. 1a). Desorption of pure HCOOH occurs at 142 and 166 K under our experimental conditions (solid line), while HCOOH in H$_2$O desorbs together with H$_2$O between 150 and 160 K (dashed line) (Fig. 1c). This is the desorption temperature range found in the co-deposition experiment for mass 46 amu (Fig. 1a). Similar TPD experiments using pure H$_2$CO ice and H$_2$CO in H$_2$O ice reveal no desorption peaks for mass 46 amu (Fig. 1b). For this we conclude that the signal from mass 46 amu detected during the TPD of the co-deposition experiment corresponds to HCOOH desorption from a polar ice and that all detected HCOOH originates from surface reactions.

The 30 amu mass signal (right-hand column) in the TPD curve from the co-deposition experiment presents a double peak at 147 and 160 K (Fig. 1a). Desorption of pure H$_2$CO occurs at 95 K, while H$_2$CO in H$_2$O desorbs at 97 and 148 K, which is close to one of the desorption temperatures found in the co-deposition experiment. In a TPD experiment of pure HCOOH, the 30 amu mass signal is detected at the same temperature found for mass 46 amu, showing that HCOOH can be fragmented into H$_2$CO by the electron-emitting filament in the ionization chamber of the QMS. In the TPD curve of solid HCOOH in H$_2$O, the 30 amu mass signal peaks at 148 K, which is the same desorption temperature of H$_2$CO in H$_2$O. Hence, when HCOOH ice is diluted in H$_2$O, some

of it is already dissociated in the solid phase to form H$_2$CO at high temperatures.

In conclusion, we find that HCOOH is formed in the solid phase for temperatures between the co-deposition of H atoms and CO:O$_2$ mixtures at 15 K and its desorption at ~160 K. In the following sections we will use IR data to constrain the temperature of HCOOH formation and its reaction pathway.

3.2 Formation temperature

As a first step in the IR data analysis, a straight baseline is subtracted from all spectra. HCOOH ice presents several absorption features in the spectral range from 2000 to 1000 cm^{-1}, among which the ν(CO) stretching mode at ~1700 cm^{-1} is the strongest one. Shape and position of the HCOOH IR spectral features are sensitive to temperature and ice composition as was shown by Bisschop et al. (2007a). In order to further investigate the temperature at which HCOOH ice is formed, we have compared the IR spectra acquired during the TPD of the co-deposition experiments to selected laboratory spectra in the range between 1000 and 2000 cm^{-1}. We will start close to the HCOOH desorption temperature since the QMS recorded TPD results gave a positive identification of HCOOH there and we will then go down in temperature to detect the first occurrence of HCOOH. The top-left side of Fig. 2 shows the RAIR spectrum at 150 K of a H-atom and CO:O$_2$ = 4:1 co-deposition experiment. The broad 1720 cm^{-1} HCOOH stretching mode overlaps with the 1650 cm^{-1} H$_2$O bending mode. Solid H$_2$O$_2$ appears also in the investigated spectral range as a strong and broad absorption. The top-right side of Fig. 2 shows the zoom-in of the RAIR spectrum in the range between 1450 and 1850 cm^{-1}. In the same panel a broad component at 1720 cm^{-1} from the HCOOH:H$_2$O = 1:10 mixture at 50 K is plotted (dotted line with an offset). This feature not only reproduces the band profile and peak position of the HCOOH stretching mode, but also indicates that HCOOH is mixed with H$_2$O in the ice at temperatures slightly below the HCOOH desorption temperature,
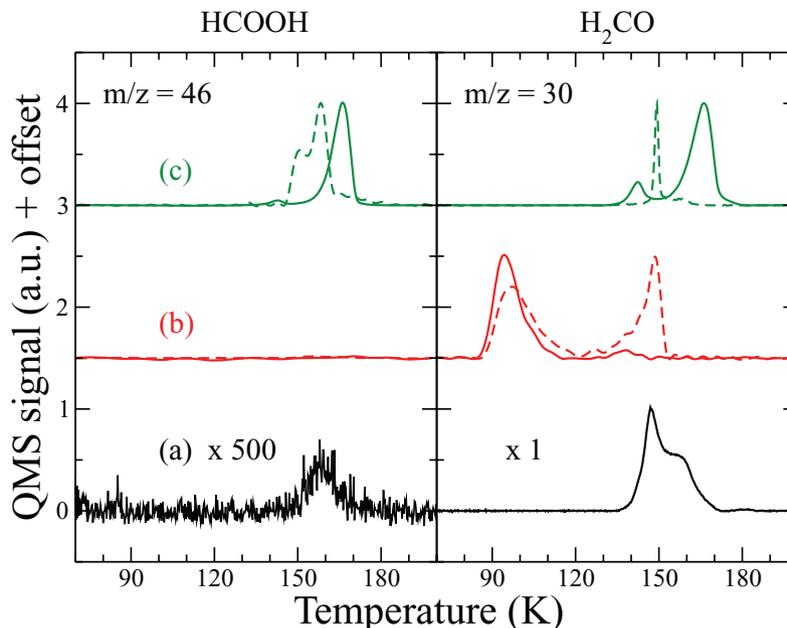
Figure 1. The 46 amu (HCOOH, left − hand column) and 30 amu mass QMS signals (H$_2$CO, right − hand column) from the TPD of a H-atom and CO:O$_2$ = 4:1 co-deposition experiment (a), compared to TPDs of the following experiments: solid H$_2$CO (b, solid line), H$_2$O:H$_2$CO = 3:1 mixture (b, dashed line) and HCOOH ice (c, solid line), H$_2$O:HCOOH = 10:1 mixture (c, dashed line). Spectra are offset for clarity.
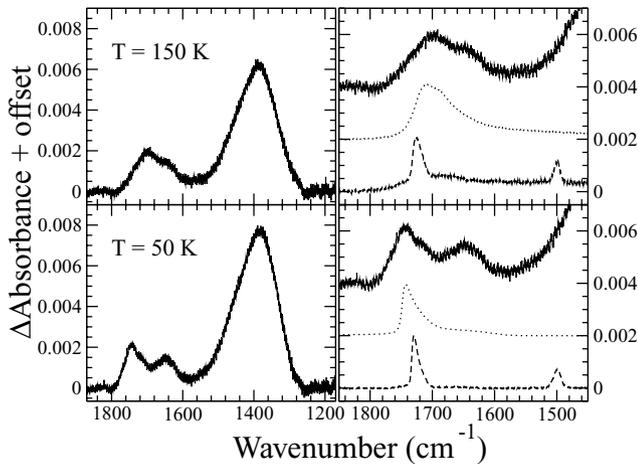
Figure 2. IR spectra at 150 K (top panels) and 50 K (bottom panels) from the H-atom and CO:O_2 = 4:1 co-deposition experiment (solid lines). The left-hand side of the figure shows the spectra in the range between 1000 and 2000 cm^{-1}, while the right-hand side shows a zoom-in of the 1700 cm^{-1} region. For comparison two spectra of mixed H_2O:HCOOH = 10:1 (dotted line) and H_2O:H_2CO = 3:1 (dashed line) are shown in the top-right panel, and two spectra of pure HCOOH (dotted line) and H_2CO (dashed line) are plotted in the bottom-right panel. Spectra are offset for clarity.

confirming the mass spectrometry analysis presented in Section 3.1. A H_2CO:H_2O = 1:3 mixture spectrum at 50 K (dashed line) is also plotted to show how shape and position of H_2CO ν(CO) stretching mode differ from the 1720 cm^{-1} spectral feature.

The bottom-left panel of Fig. 2 shows the IR spectrum at 50 K of the same H-atom and CO:O_2 = 4:1 co-deposition experiment, while the bottom-right panel of Fig. 2 plots the zoom-in of the aforementioned spectrum and the 1740 cm^{-1} feature from a pure HCOOH ice at 30 K (dotted line), compared to a spectrum of pure H_2CO at 50 K (dashed line). The HCOOH feature present in our IR spectrum at 50 K is narrow and shifted to higher wavenumbers with respect to the 1650 cm^{-1} H_2O bending mode. Again, shape and peak position are better reproduced by the HCOOH than by H_2CO, since the H_2CO band peaks at 1730 cm^{-1} and is more narrow than the HCOOH feature. This result indicates that HCOOH is present in the ice at 50 K and is most likely formed at lower temperatures. It is also less mixed with H_2O ice than at high temperatures. Hence, at high temperatures HCOOH molecules can better diffuse in the ice and get mixed with H_2O_2 and H_2O ice above 100 K, when H_2O ice starts restructuring.

Fig. 3(a) shows the IR spectrum of the ice after co-deposition of H atoms and CO:O_2 = 4:1 at 15 K, when the ice is hydrogenated but not yet heated. At this stage of the experiment the HCOOH stretching mode is around our detection limit and a feature at 1815 cm^{-1} is detected. The identification of this feature will be discussed in Section 3.3. The first clear detection of solid HCOOH in the CO:O_2 = 4:1 experiment is shown in Fig. 3(b) at ∼30 K, when CO and O_2 are not completely desorbed yet from the ice (Öberg et al. 2005; Acharyya et al. 2007). At this temperature the 1815 cm^{-1} intensity decreases and the band broadens and shifts to 1820 cm^{-1}, while the HCOOH stretching mode appears at ∼1750 cm^{-1}. The HCOOH peak position and band shape are in agreement with those from a CO:HCOOH = 100:1 mixture shown in Fig. 3(c). Solid HCOOH is detected at 15 K in the co-deposition experiments of H atoms and CO:O_2 = 1:1 and 1:4 (spectra not shown). However, the feature at 1815 cm^{-1} is detected only in the H-atom and CO:O_2 = 1:1 co-deposition experiment, where an increase of the HCOOH stretching
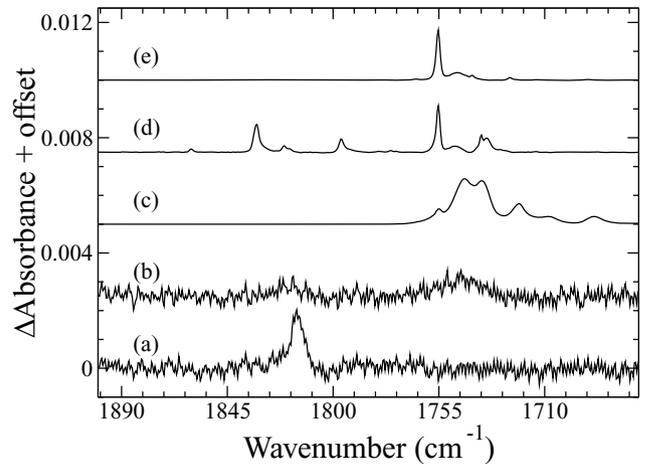
Figure 3. IR spectra from a H-atom and CO:O_2 = 4:1 co-deposition experiment at 15 K (a) and 30 K (b) compared to a spectrum of CO:HCOOH = 100:1 at 15 K (c), CO:HCOOH = 1000:1 at 15 K (d), and a spectrum from a CO:O_2 = 100:1 co-deposition experiment at 15 K (e) using higher H-atom flux (2×10^{14} cm^{-2} s^{-1}) and CO:O_2 flow (1×10^{14} cm^{-2} s^{-1}). Spectra are offset for clarity.

mode is observed at 30 K, in agreement with the results from the CO:O_2 = 4:1 mixture shown in Fig. 3. In the case of the CO:O_2 = 1:4 mixture we do not observe the feature at 1815 cm^{-1} at 15 K and the increase of the HCOOH stretching mode at 30 K. Thus, the 1815 cm^{-1} feature requires the presence of CO in the mixture. Figs 3(d) and (e) will be discussed in the next section.

As the previous discussion showed, the HCOOH feature changes strongly in shape and position as a function of temperature. This is generally true for the entire spectrum. Fig. 4 shows this clear temperature dependence in the morphology of the ice in a CO:O_2 = 4:1 co-deposition experiment after an H-atom fluence of 2.7×10^{17} atoms cm^{-2}. In a CO- and O_2-*rich* environment, like the ice at 15 K of our co-deposition experiments, the H_2O_2 and H_2O IR bands are present in both hydrophobic and hydrophilic contributions (monomer and bulk, respectively; see Fig. 4a). For feature assignments see Cuppen et al. 2010, and references therein. By increasing the temperature of the sample, the amount of hydrophobic material decreases and the H_2O_2 and H_2O bands broaden and shift. Thus, the 50 K IR spectrum presents several broad bulk features originating
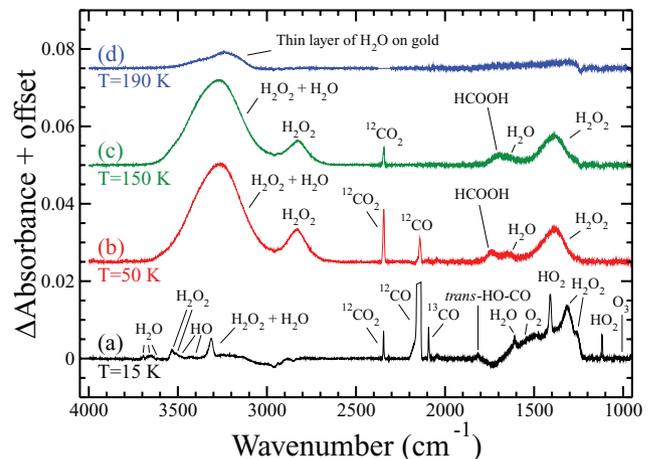
Figure 4. The 15 K (a), 50 K (b), 150 K (c) and 190 K (d) IR spectra of the H-atom and CO:O_2 = 4:1 co-deposition experiment after an H-atom fluence of 2.7×10^{17} atoms cm^{-2}. Spectra are offset for clarity.

from species like H_2O_2, H_2O, and bands due to CO_2, HCOOH and traces of CO, still trapped in the mixture (Fig. 4b). In the 150 K spectrum (Fig. 4c) the CO stretching mode has disappeared, traces of solid CO_2 are present in the ice, since a very weak stretching mode band is still visible, and the HCOOH 1740 cm^{-1} feature has broadened and shifted towards lower wavenumbers (1700 cm^{-1}), overlapping with the 1650 cm^{-1} H_2O bending mode. The HCOOH feature decreases in the RAIR spectra at the same temperature where the signal of mass 46 amu increases in the mass spectrometer ($\sim$160 K; see Fig. 1a).

In conclusion, the results presented here show that HCOOH ice is formed during co-deposition experiments at low temperature ($\sim$15 K) and that its formation increases at a temperature close to the desorption temperature of volatile species like CO, O_2, when radicals produced by the hydrogenation of the ice are more mobile ($\sim$30 K). In the next section we describe the possible reaction mechanism.

3.3 Possible reaction pathways

IR spectroscopy is used to identify the possible reaction intermediates: HCO according to reactions (1) and (2) or HO–CO according to reaction (3).

As mentioned in Section 2, the deposited ice mainly consists of CO and O_2 molecules. This is reflected by the saturated CO stretching band mode present in Fig. 4(a) and a very weak O_2 absorption band peaking at 1550 cm^{-1} (the presence of O_2 in the ice causes also distortions in the IR spectrum, as discussed by Cuppen et al. 2010). The IR spectrum at 15 K presents a forest of bands in absorption due to newly formed species upon hydrogenation of O_2 ice, like H_2O_2, H_2O, HO_2, OH (see Cuppen et al. 2010). CO ice is not hydrogenated in our experiments, since neither HCO, H_2CO nor CH_3OH features appear in the RAIR spectra at 15 K (Fig. 4a). This is consistent with a previous conclusion that CO + H is less efficient than O_2 + H (Fuchs et al. 2009; Cuppen et al. 2010; Ioppolo et al. 2010). Therefore, since HCO and H_2CO never form in the other co-deposition experiments, reactions (1) and (2), with HCO as intermediate, are likely not to take place during our co-deposition experiments.

We performed a control co-deposition experiment, using higher H-atom flux (2×10^{14} cm^{-2} s^{-1}) and higher CO:O_2 = 100:1 deposition rate ($\sim$1 $\times 10^{14}$ cm^{-2} s^{-1}), with the intention to give an assignment to the low-temperature 1815 cm^{-1} feature. This experiment allows to observe more reactions products, but with similar matrix properties to the other co-deposition experiments. During this control experiment several species, like OH, HO_2, H_2O, H_2O_2, O_3, CO_2, CO_3, HO–CO, HCOOH, HCO, H_2CO are formed in the ice at 15 K. Table 1 lists the assignments of the features present in the spectral region between 1700 and 1900 cm^{-1}, also shown in Fig. 3(d). The band position and shape of solid HCOOH formed at low temperature in the control experiment corresponds to the HCOOH feature in a CO matrix (CO:HCOOH = 1000:1) as shown in Fig. 3(e). The *cis* and *trans*-HO–CO complexes appear in the control experiment spectrum in both environments: polar (in H_2O matrix at 1775 and 1820 cm^{-1}, respectively) and apolar ice (in CO matrix at 1796 and 1833 cm^{-1}, respectively). The peak at 1815 cm^{-1} is detected in our standard co-deposition experiments and can now be assigned by comparison with the control experiment results to the stabilised *trans*-HO–CO complex in a polar environment. The *cis*-HO–CO complex absorption strength, which is normally weaker than that from the *trans*-HO–CO, is around the detection limit.

Table 1. Assigned IR features with their corresponding reference in the range between 1700 and 1900 cm^{-1} as found in a control co-deposition experiment.

Species	Position (cm^{-1})	Reference	Matrix
HCO	1860	Milligan & Jacox (1964)	Ar
trans-HO–CO	1833	Milligan & Jacox (1971)	CO
trans-HO–CO	1820	Zheng & Kaiser (2007)	H_2O
cis-HO–CO	1796	Milligan & Jacox (1971)	CO
cis-HO–CO	1775	Zheng & Kaiser (2007)	H_2O
HCOOH	1755	This work	CO
HCOOH	1748	This work	CO
H_2CO	1737	Nelander (1980)	N_2
H_2CO	1734	Nelander (1980)	N_2

Solid HCOOH is therefore most likely formed through reaction (3), which can also lead to the formation of CO_2 + H_2 and H_2O + CO (Goumans et al. 2008). The presence of CO_2 ice and the stabilised *trans*-HO–CO complex at 1815 cm^{-1} (Fig. 4), suggests indeed that CO ice can react with OH-bearing species produced by hydrogenation of O_2 ice, since this bond is only present after hydrogenation of CO and O_2 containing ices. As previously discussed, the HO–CO complex is only detected in a water-rich environment. However, our ice is mainly composed of CO and O_2, with traces of other polar species. Therefore, we would expect to detect the HO–CO complex also in a water-*poor* environment. Moreover, the amount of solid HCOOH detected at 15 K is close to the detection limit for all the mixtures investigated, while CO_2 is on average 10 times more abundant than HCOOH in the ice at low temperature. These experimental results suggest that the HO–CO complex formed in a CO and O_2 matrix is mainly used to form CO_2 by direct dissociation of the complex, and only a small fraction of CO_2 comes from reaction (3) at 15 K. Furthermore, the HO–CO complex appears to be stabilized and shielded from hydrogenation in a water-*rich* environment at low temperatures. It is indeed likely that H-bonding improves coupling and heat dissipation through the ice, which would stabilize the HO–CO complex more easily in a water-*rich* environment than in a CO and O_2 ice (Goumans, private communication). The HO–CO intermediate formed in a polar ice is then available again to react at higher temperatures, when it is more mobile and hydrogen can still be present in the ice. In our experiments also solid H_2CO_3 can be formed from the same HO–CO complex through the reaction:

$$CO + OH \rightarrow HO–CO \overset{OH}{\rightarrow} H_2CO_3, \qquad (4)$$
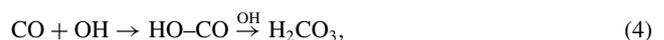
as shown by Oba et al. (2010). Moreover, reaction (4) can also lead to the formation of CO_2 + H_2O and H_2O_2 + CO. At temperatures below 100 K the HCOOH ν(CO) stretching mode overlaps with the H_2CO_3 one, hindering a spectral assignment of solid H_2CO_3 in the IR spectra. However, the different desorption temperatures of these molecules allow an identification, since HCOOH desorbs at $\sim$160 K and H_2CO_3 at $\sim$250 K.

Fig. 4(d) shows the 190 K RAIR spectrum from the co-deposition experiment, in which all the absorption bands have disappeared. Distortions at low wavenumbers in the difference RAIR baseline spectrum are caused by the high temperature of the gold substrate. This result excludes the presence of formed solid H_2CO_3 in the ice in our co-deposition experiments, since H_2CO_3 desorbs at temperatures above 220 K (e.g. Zheng & Kaiser 2007) and should therefore still be present at 190 K.

Oba et al. (2010) studied the formation of solid CO_2 through surface reactions between carbon monoxide and non-energetic OH radicals, produced by dissociating H_2O molecules in microwave-induced plasma. According to their results H_2CO_3 was formed through reaction (4), but no HCOOH was detected. The difference in the experimental results between Oba et al. (2010) and this work can be found in a different flux composition. In their case, H_2O is dissociated and a combination of OH radicals and H atoms gives the final flux, most likely one to one. In the present work we use an H-atom flux. The OH radicals present in the ice are formed via surface reactions. Hence, the HO–CO complex has a higher probability to find and react with a H atom instead of a OH radical, which is less abundant in the ice.

3.4 Branching ratio of reaction HO–CO + H

As shown in the previous sections, solid CO_2 and H_2O, which are also observed in our IR spectra, can be formed together with HCOOH by reaction HO–CO + H (Goumans et al. 2008). However, the determination of the branching ratios for this reaction is not straightforward, since CO_2 can also be formed during co-deposition by direct dissociation of the complex HO–CO (Oba et al. 2010), and H_2O through hydrogenation of molecular oxygen (Ioppolo et al. 2008; Miyauchi et al. 2008; Oba et al. 2009; Cuppen et al. 2010; Ioppolo et al. 2010). Here we make an attempt to estimate the branching ratios of reaction HO–CO + H at higher temperatures, when the other reaction routes to form CO_2 and H_2O are less efficient. At 50 K the three reaction products are all formed but have not yet desorbed from the ice. In order to calculate the branching ratios based on our experimental results, we assume that

(i) solid HCOOH is formed only through reaction (3);

(ii) the CO_2 formed at 15 K comes mainly through direct dissociation of the complex HO–CO in a water-*poor* environment and, therefore, is subtracted to the CO_2 column density obtained at 50 K;

(iii) H_2O can be formed through hydrogenation of O_2 and, therefore, the contribution of this channel is estimated by comparing the results presented here to those from a similar experiment ($H/O_2 = 10$) shown by Cuppen et al. (2010) and then subtracted to the H_2O column density obtained in our 50 K spectrum.

Since literature values of transmission band strengths cannot be used directly in reflectance measurements, an apparent absorption strength of HCOOH, CO_2 and H_2O is calculated from calibration experiments. The determination of this apparent absorption strength is set-up specific. The calibration method is described in Fuchs et al. (2009) and Ioppolo et al. (2010).

The values for the branching ratios obtained here after subtracting the contributions from other possible reaction channels are in agreement with those presented by Goumans et al. (2008), who suggested that the branching ratio is purely statistical:

$$CO + OH \xrightarrow{H} \begin{cases} HCOOH & k, \\ CO_2 + H_2 & (0.7 \pm 0.3)k, \\ H_2O + CO & \leq k, \end{cases} \quad (5)$$
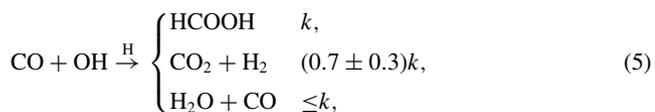
where k is the branching ratio of the channel leading to HCOOH. We conclude from the 50 K IR spectrum that the amount of solid HCOOH and CO_2 formed in our standard H-atom and $CO:O_2 = 4:1$ co-deposition experiment is $\sim 1 \pm 0.1$ ML, while the amount of H_2O is roughly the same as that produced after the same H-atom fluence in the H-atom and O_2 co-deposition experiment ($H/O_2 = 10$) shown by Cuppen et al. (2010) ($\sim 10 \pm 1$ ML). Therefore, H_2O

ice is mainly formed through hydrogenation of O_2 and the amount of H_2O formed through reaction HO–CO + H could be equal to that of CO_2 and HCOOH within the experimental uncertainties. Results using the $CO:O_2 = 1:1$ and 1:4 mixtures confirmed the branching ratio values shown above.

4 ASTROPHYSICAL IMPLICATIONS

The origin of the observed HCOOH in the interstellar medium has been unclear. Both gas-phase reactions and grain-surface processes have been suggested for producing the HCOOH column densities observed in star-forming regions. Results from a two-stage hot-core gas-grain chemical model (stage 1: collapse; stage 2: warm-up phase) proposed by Garrod & Herbst (2006) suggested that HCOOH is mainly formed in the gas phase during the warm-up phase. According to the authors, at early times of the warm-up, HCOOH is most likely formed in the gas phase through the dissociative recombination of protonated formic acid, which forms by radiative association of HCO^+ and H_2O or by reaction $CH_4 + O_2^+$. However, as mentioned in the introduction, recent gas-phase laboratory experiments showed that the dissociative recombination channel is less efficient than considered before. In the case of L134N for instance, it is found to be eight times less efficient than in models using the latest release of the UMIST data base for astrochemistry (Woodall et al. 2007), and a factor of 4 less than the observed value. Hence, the observed HCOOH abundances in cold regions cannot be explained by gas-phase reactions only, and, therefore, surface reactions should be taken into account for the formation of HCOOH, even at low temperatures. Especially, since solid HCOOH may be destroyed by energetic processing or in reaction with NH_3 to lead to $HCOO^-$ and NH_4^+ (e.g. Hudson & Moore 1999; Schutte et al. 1999). HCOOH ice was shown in the laboratory to be stable against further hydrogenation (Bisschop et al. 2007b).

The model used by Garrod & Herbst (2006) includes only surface reaction (2). At low temperatures, the formation of formaldehyde and methanol through subsequent hydrogenation of solid CO (Fuchs et al. 2009) is favoured over the formation of HCOOH through reaction (2). We can roughly estimate the efficiency of reaction (2) at low temperatures considering the abundance of H atoms and OH radicals over CO molecules at the end of the cloud collapse phase. If we assume that one H_2O molecule is formed on the grain surface from one OH radical, which gives a ratio one-to-one between H_2O and OH, CO ice is four times less abundant on average in dense regions than OH radicals (e.g. Gibb et al. 2004). However, H atoms are orders of magnitude more abundant than OH radicals in this environment and H atoms are more mobile on the surface. Therefore, the probability that an HCO radical finds an OH to react with before it is hydrogenated is almost negligible. Garrod & Herbst (2006) found an optimum in HCOOH formation through reaction (2) at $\sim$40 K, when H_2CO resides in the gas phase, but can also accrete again on the grains and re-evaporate quickly. This allows for reaction with OH radicals in the solid phase to form HCO available for reaction (2). However, grain-surface reaction (2) was never considered as a dominant process in their model during the warm-up phase, since HCOOH can still be formed in the gas phase at these temperatures (>40 K) through the reaction OH + H_2CO.

The experiments presented here are designed to test the possible reaction channels and not necessarily to simulate a realistic interstellar ice. In particular, they show a low efficiency of reaction (2) under our laboratory conditions, and even though we do not exclude that reactions (1) and (2) can occur under interstellar conditions, our experiments show unambiguously the formation of

HCOOH through reaction (3) in the solid phase at low temperatures, giving roughly the same branching ratio for the three final reaction products (HCOOH, CO_2 and H_2O). These results are in agreement with density functional theory models, which suggest that there could be equal branching ratio between the three possible channels. Under interstellar conditions, the HO–CO complex is expected to be even more stabilized in the H_2O-*rich* ices, than in our apolar laboratory analogues. Furthermore, the HO–CO complex channel should be considered an important HCOOH formation route, since it could explain the presence of HCOOH in dense molecular clouds and at the beginning of the warm-up phase of the protostar in low- and high-mass star-forming regions.

ACKNOWLEDGMENTS

REFERENCES

Acharyya K., Fuchs G. W., Fraser H. J., van Dishoeck E. F., Linnartz H., 2007, A&A, 466, 1005

Bisschop S. E., Fuchs G. W., Boogert A. C. A., van Dishoeck E. F., Linnartz H., 2007a, A&A, 470, 749

Bisschop S. E., Fuchs G. W., van Dishoeck E. F., Linnartz H., 2007b, A&A, 474, 1061

Bisschop S. E., Jørgensen J. K., van Dishoeck E. F., de Wachter E. B. M., 2007c, A&A, 465, 913

Boogert A. C. A. et al., 2004, ApJS, 154, 359

Boogert A. C. A. et al., 2008, ApJ, 678, 985

Bottinelli S., Ceccarelli C., Williams J. P., Lefloch B., 2007, A&A, 463, 601

Cuppen H. M., Ioppolo S., Romanzin C., Linnartz H., 2010, Phys. Chemistry Chemical Phys. (doi: 10.1039/C0CP00251H)

Fuchs G. W., Cuppen H. M., Ioppolo S., Bisschop S. E., Andersson S., van Dishoeck E. F., Linnartz H., 2009, A&A, 505, 629

Garrod R. T., Herbst E., 2006, A&A, 457, 927

Gibb E. L. et al., 2000a, ApJ, 536, 347

Gibb E. L., Nummelin A., Irvine W. M., Whittet D. C. B., Bergman P., 2000b, ApJ, 545, 309

Gibb E. L., Whittet D. C. B., Boogert A. C. A., Tielens A. G. G. M., 2004, ApJS, 151, 35

Goumans T. P. M., Uppal M. A., Brown W. A., 2008, MNRAS, 384, 1158

Hudson R. L., Moore M. H., 1999, Icarus, 140, 451

Ikeda M., Ohishi M., Nummelin A., Dickens J. E., Bergman P., Hjalmarson Å., Irvine W. M., 2001, ApJ, 560, 792

Ioppolo S., Cuppen H. M., Romanzin C., van Dishoeck E. F., Linnartz H., 2008, ApJ, 686, 1474

Ioppolo S., Cuppen H. M., Romanzin C., van Dishoeck E. F., Linnartz H., 2010, Phys. Chemistry Chemical. Phys. (doi:10.1039/C0CP00250J)

Irvine W. M., Friberg P., Kaifu N., Matthews H. E., Minh Y. C., Ohishi M., Ishikawa S., 1990, A&A, 229, L9

Knez C. et al., 2005, ApJ, 635, L145

Leung C. M., Herbst E., Huebner W. F., 1984, ApJS, 56, 231

Liu S.-Y., Mehringer D. M., Snyder L. E., 2001, ApJ, 552, 654

Liu S.-Y., Girart J. M., Remijan A., Snyder L. E., 2002, ApJ, 576, 255

Milligan D. E., Jacox M. E., 1964, J. Chemical Phys., 41, 3032

Milligan D. E., Jacox M. E., 1971, J. Chemical Phys., 54, 927

Miyauchi N., Hidaka H., Chigai T., Nagaoka A., Watanabe N., Kouchi A., 2008, Chemical Phys. Lett., 456, 27

Nelander B., 1980, J. Chemical Phys., 73, 1034

Oba Y., Miyauchi N., Hidaka H., Chigai T., Watanabe N., Kouchi A., 2009, ApJ, 701, 464

Oba Y., Watanabe N., Kouchi A., Hama T., Pirronello V., 2010, ApJ, 712, L174

Öberg K. I., van Broekhuizen F., Fraser H. J., Bisschop S. E., van Dishoeck E. F., Schlemmer S., 2005, ApJ, 621, L33

Öberg K. I., Garrod R. T., van Dishoeck E. F., Linnartz H., 2009, A&A, 504, 891

Requena-Torres M. A., Martín-Pintado J., Rodríguez-Franco A., Martín S., Rodríguez-Fernández N. J., de Vicente P., 2006, A&A, 455, 971

Schutte W. A., Greenberg J. M., van Dishoeck E. F., Tielens A. G. G. M., Boogert A. C. A., Whittet D. C. B., 1998, Ap&SS, 255, 61

Schutte W. A. et al., 1999, A&A, 343, 966

Tielens A. G. G. M., Hagen W., 1982, A&A, 114, 245

Tschersich K. G., von Bonin V., 1998, J. Applied Phys., 84, 4065

Tschersich K. G., 2000, J. Applied Phys., 87, 2565

Tschersich K. G., Fleischhauer J. P., Schuler H., 2008, J. Applied Phys., 104, 034908

van Dishoeck E. F., Blake G. A., Jansen D. J., Groesbeck T. D., 1995, ApJ, 447, 760

Vigren E. et al., 2010, ApJ, 709, 1429

Watanabe N., Nagaoka A., Hidaka H., Shiraki T., Chigai T., Kouchi A., 2006, Planet. Space Sci., 54, 1107

Winnewisser G., Churchwell E., 1975, ApJ, 200, L33

Woodall J., Agúndez M., Markwick-Kemper A. J., Millar T. J., 2007, A&A, 466, 1197

Zheng W., Kaiser R. I., 2007, Chemical Phys. Lett., 450, 55

Zuckerman B., Ball J. A., Gottlieb C. A., 1971, ApJ, 163, L41

This paper has been typeset from a TEX/LATEX file prepared by the author.